Structural Effects of Fibulin 5 Missense Mutations Associated with Age-Related Macular Degeneration and Cutis Laxa

Richard P. O. Jones,[*,1] Caroline Ridley,[2] Thomas A. Jowitt,[2] Ming-Chuan Wang,[2] Marjorie Howard,[2] Nicoletta Bobola,[3] Tao Wang,[1] Paul N. Bishop,[1,2] Cay M. Kielty,[2] Clair Baldock,[2] Andrew J. Lotery,[4] and Dorothy Trump*[*,1]

Purpose. AMD has a complex etiology with environmental and genetic risk factors. Ten fibulin 5 sequence variants have been associated with AMD and two other fibulin 5 mutations cause autosomal-recessive cutis laxa. Fibulin 5 is a 52-kDa calcium-binding epidermal growth factor (cbEGF)–rich extracellular matrix protein that is essential for the formation of elastic tissues. Biophysical techniques were used to detect structural changes in the fibulin 5 mutants and to determine whether changes are predictive of pathogenicity.

Methods. Native PAGE, nonreduced SDS-PAGE, size-exclusion column multiangle laser light scattering, sedimentation velocity, and circular dichroism (CD) were used to investigate the mobility, hydrodynamic radii, folding, and oligomeric states of the fibulin 5 mutants in the absence and presence of Ca^{2+}.

Results. CD showed that all mutants are folded, although perturbations to secondary structure contents were detected. Both cutis laxa mutants increased dimerization. Most other mutants slightly increased self-association in the absence of Ca^{2+} but this was also demonstrated by G202R, a polymorphism detected in a control individual. The AMD-associated mutant G412E showed lower-than-expected mobility during native-PAGE, the largest hydrodynamic radius for the monomer form and the highest levels of aggregation in both the absence and presence of Ca^{2+}.

Conclusions. The results identified structural differences for the disease-causing cutis laxa mutants and for one AMD variant (G412E), suggesting that this may also be pathogenic. Although the other AMD-associated mutants showed no gross structural differences, they cannot be excluded as pathogenic by differences outside the scope of this study—for example, disruption of heterointeractions. (*Invest Ophthalmol Vis Sci.* 2010;51: 2356–2362) DOI:10.1167/iovs.09-4620

Age related macular degeneration (AMD) has a complex etiology with both environmental risk factors[1,2] and genetic associations with complement factors[3–7] and the chromosome 10 locus *LOC387715*.[8] In addition, 10 heterozygous missense fibulin 5 variants (V60L, R71Q, P87S, Q124P, V126M, I169T, G267S, R351W, A363T, and G412E; Fig. 1) have been identified in AMD patients but not in control subjects, and the variant G202R has been found in one control.[9,10] Each variant occurred in only one person, and the corresponding WT fibulin 5 residue was conserved across species.[9,10] A further two missense fibulin 5 mutations (C217R and S227P) are known to cause the autosomal recessive disease cutis laxa.[11–13]

Genetic studies of a complex disease can indicate associations between the disease and sequence variants within a candidate gene, and it can be difficult to determine whether the sequence changes confer increased disease susceptibility or the association has occurred by chance. This contrasts with the situation for monogenic disorders in which a pathogenic mutation is enough to cause the disease phenotype by altering the function of the gene or protein. We were interested in comparing the effects on fibulin 5 of the pathogenic cutis laxa mutations and the sequence variants associated with AMD.

The fibulins are seven extracellular matrix proteins that contain tandem calcium-binding epidermal growth factor domains (cbEGFs). Fibulin 5 (Fig. 1) is a 52-kDa protein containing a modified N-terminal cbEGF domain, followed by five cbEGF domains, and a fibulin-type C-terminal module.[14] All its 34 cysteines are thought to be internally disulfide bonded.[15] Wild-type (WT) fibulin 5 exists primarily as an L-shaped monomer in the absence of Ca^{2+} and as a donut-shaped dimer in the presence of extracellular physiological Ca^{2+} concentrations.[16] Fibulins are involved in the assembly, organization, and stabilization of macromolecular complexes.[17] Fibulin 5 is expressed by elastin-rich tissues,[18,19] including the retinal pigmented epithelium (RPE)[10] and is essential for elastinogenesis. The fibulin 5-knockout mouse exhibits severe elastinopathy, with loose skin, vascular abnormalities, and emphysematous lungs.[20,21] A single mutation in fibulin 3 (also known as *EFEMP1*) causes the dominant disease Malattia Leventinese (Doyne's honeycomb retinal dystrophy), and the similarity between AMD and this retinal phenotype led to the initial study of fibulins in AMD and the first association of sequence variants in fibulin 5.[10]

From [1]Genetic Medicine, Manchester Academic Health Science Centre, Central Manchester University Hospitals NHS Foundation Trust, [2]Wellcome Trust Centre for Cell-Matrix Research, Faculty of Life Sciences, and [3]School of Dentistry, Faculty of Medical and Human Sciences, University of Manchester, Manchester, United Kingdom; and [4]Clinical Neurosciences Division, University of Southampton, Southampton, United Kingdom.

Supported by Wellcome Trust Grants 123364 (DT, AJL, PNB CMK, RPOJ, CR), 072291 (CB, MCW) and VIP award (NB, RPOJ & DT); and the National Institutes of Health Research (NIHR) Manchester Biomedical Research Centre.

Submitted for publication September 9, 2009; revised October 26, 2009; accepted November 24, 2009.

Disclosure: **R.P.O. Jones**, None; **C. Ridley**, None; **T.A. Jowitt**, None; **M.-C. Wang**, None; **M. Howard**, None; **N. Bobola**, None; **T. Wang**, None; **P.N. Bishop**, None; **C.M. Kielty**, None; **C. Baldock**, None; **A.J. Lotery**, None; **D. Trump**, None

* Each of the following is a corresponding author: Dorothy Trump, Genetic Medicine, University of Manchester, Manchester Academic Health Science Centre, Central Manchester University Hospitals NHS Foundation Trust, St. Mary's Hospital, Oxford Road, Manchester, M13 9WL, UK; dorothy.trump@manchester.ac.uk.

Richard P. O. Jones, Genetic Medicine, University of Manchester, Manchester Academic Health Science Centre, Central Manchester University Hospitals NHS Foundation Trust, St. Mary's Hospital, Oxford Road, Manchester, M13 9WL, UK; rpojones@yahoo.co.uk.

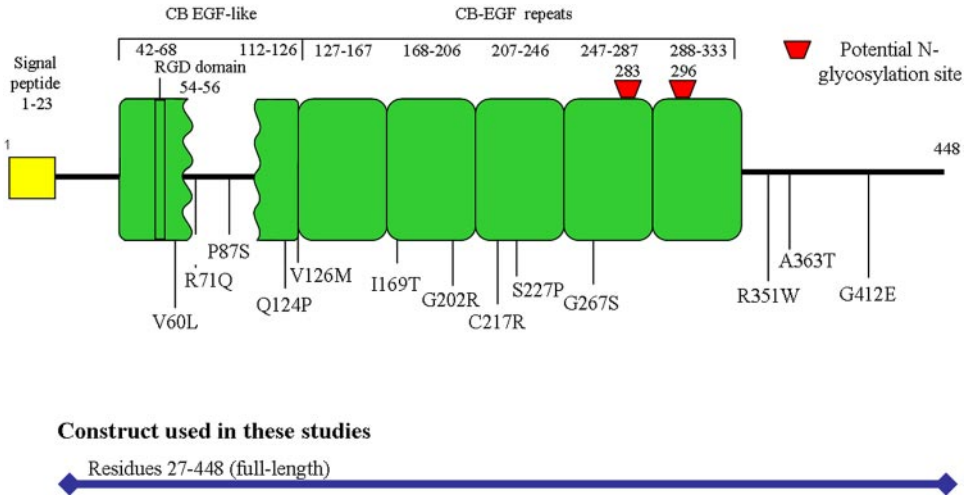

FIGURE 1. Diagram of fibulin 5 showing the location of the cbEGF domains, potential glycosylation sites, and mutations associated with cutis laxa (C217R and S227P) and age-related macular degeneration (V60L, R71Q, P87S, Q124P, V126M, I169T, G267S, R351W, A363T, and G412E). G202R is a polymorphism that was found in a control rather than in a patient.

Our hypothesis was that the fibulin 5 sequence variants lead to increased susceptibility to AMD by altering the structure of the fibulin 5 protein. We used a variety of biophysical techniques to detect structural changes in fibulin 5 mutants and to determine whether the results could help to predict the pathogenicity of the AMD-associated sequence changes by comparing results with those from the cutis laxa mutants. We have previously shown that the two cutis laxa mutants and four of the AMD-associated variants (G412E, G267S, I169T, and Q124P) are poorly secreted,[9] and structural changes in the protein could account for this. Structural differences could also suggest a potential loss of function for those AMD-associated mutants that are secreted normally.

We investigated the two cutis laxa mutations that are known to cause disease, the G202R polymorphism that does not cause a disease, the 10 AMD variants, and the mutation R54A that should prevent binding of the fibulin 5 RGD motif (residues 54-56) to integrins, but is not associated with disease. We used EBNA 293 cells and the pCepHis vector to ensure that all mutants were secreted, followed by Ni^{2+}-affinity chromatography for protein purification. We used a combined strategy of SEC-MALLS (size exclusion column followed by multiangle laser light scattering), sedimentation velocity, CD (circular dichroism), protein homology modeling, native-PAGE, and nonreduced SDS-PAGE, to determine the shapes, hydrodynamic radii, and secondary structure content of both monomeric and dimeric forms, and levels of self-association, for these purified fibulin 5 mutants.

METHODS

Molecular Biology and Expression and Purification of Recombinant Fibulin 5 Polypeptides

Site-directed mutants were obtained (QuikChange method; Stratagene, La Jolla, CA) by using the pCepHis construct encoding wild-type fibulin 5 (residues 27-448)[22,23] as a template and the primers listed (Supplementary Fig. S1; all Supplementary Figures available at http://www.iovs.org/cgi/content/full/51/5/2356/DC1). Mutations were confirmed by DNA sequencing.

WT and mutants of fibulin 5 were expressed by EBNA 293 cells stably transfected with pCepHis constructs and secreted into serum-free medium (SAFC Biosciences, Lenexa, KS). Fibulin 5 polypeptides were purified from medium to homogeneity by Ni^{2+}-affinity chromatography.[16] The presence of fibulin 5 polypeptides and the absence of impurities in Ni^{2+}-affinity column elution fractions were demonstrated by SDS-PAGE, followed by staining with Coomassie blue and Western blot analysis (anti-3-his. antibody; Sigma-Aldrich, St. Louis, MO).[16]

Statistical Analysis

The appropriate statistical method for the analysis of single measurements for multiple mutants is Chebyshev's inequality[24] $P(x - \mu \geq \delta \cdot SD) \leq 1/\delta^2$: The probability ($P$) that a single measurement (x) for a mutant is greater than a number (δ) times the standard deviation (SD) for WT from the mean (μ) for WT is less than $1/\delta^2$. For the SEC-MALLS, sedimentation velocity and CD experiments, measurements for three or five batches of WT protein and $\delta = 4.47$ were used to construct the confidence interval $\mu \pm 4.47$ SD. This gives $P \leq 0.05$ that a single measurement for a mutant lays outside this confidence interval for WT.

Size-Exclusion Column-Multiangle Laser Light Scattering

Ni^{2+}-affinity column elution fractions containing pure fibulin 5 polypeptides were applied to a size exclusion column (Superdex 200 SEC; GE Healthcare, Piscataway, NJ) equilibrated in either buffer A (10 mM Tris [pH 7.4], 0.5 M NaCl, 2 mM EDTA, and 2 mM EGTA) or buffer B (10 mM Tris [pH 7.4], 0.5 M NaCl, and 2 mM $CaCl_2$). A high salt concentration was used to reduce amounts of aggregated polypeptides that elute in the SEC void volume.[16] The SEC eluate passed through an 18-angle MALLS detector equipped with a 688-nm laser, to determine masses, a quasi-elastic light-scattering detector (QELS) to determine hydrodynamic radii, and an r-EX refractometer to determine differential refractive index (DRI, a measure of protein concentration; all from Wyatt Technology Corp., Santa Barbara, CA). The resulting DRI, MALLS, and QELS chromatograms were baseline corrected.

Pure fibulin 5 proteins (three batches of WT; two batches for G202R, C217R, and G412E; and one batch for the other 11 mutants) were applied to the SEC equilibrated in the absence of Ca^{2+} (buffer A, Fig. 2A). Figure 2A shows the mean DRI chromatogram (black line) for WT. The maxima of peaks due to monomeric protein[16] were normalized to unity and aligned at 14 mL to compare peak shapes.

Fibulin 5 proteins (five batches of WT and one batch for each of the 14 mutants) were also analyzed by SEC in the presence of 2 mM Ca^{2+} (buffer B, Fig. 2B). Figure 2B shows the mean DRI chromatogram (black line) for WT. In Figures 2B–D, each peak maximum was normalized to unity, and the column void peak maxima (not shown) were aligned at 8.25 mL, to enable comparison of peak positions.

SEC elution fractions containing fibulin 5 monomers in the absence of Ca^{2+} and dimers in the presence of Ca^{2+} were identified and analyzed by velocity sedimentation and CD.

Sedimentation Velocity

This technique measures the velocity at which proteins move through a buffer of known composition in response to a centrifugal force. Experiments were performed in an Optima XL-A analytical ultracentri-

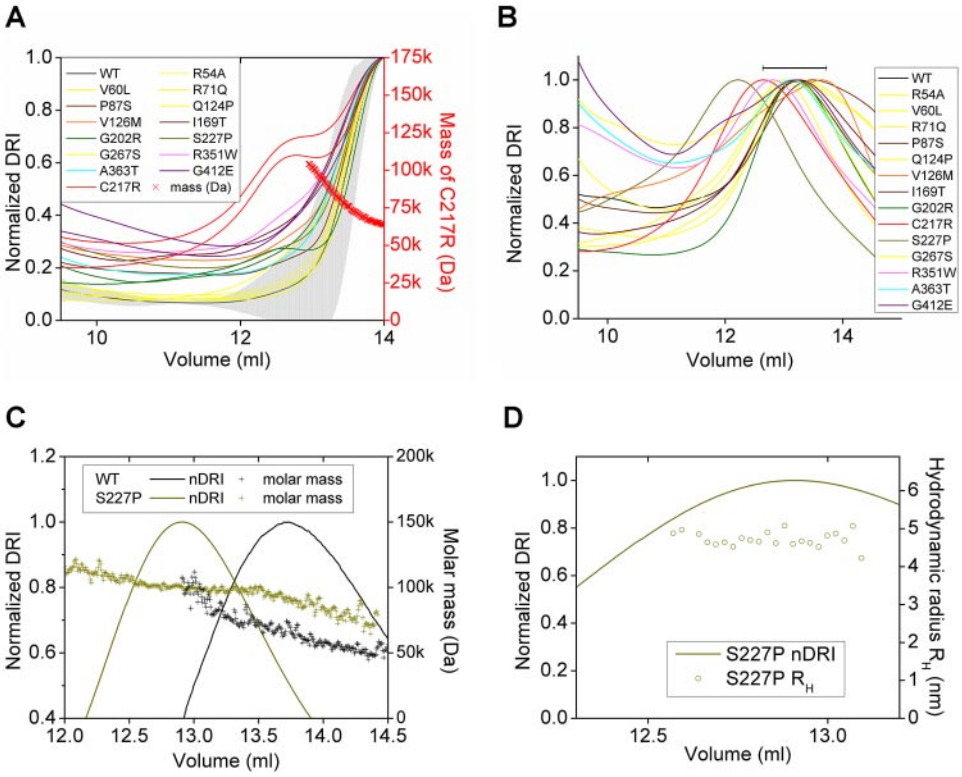

FIGURE 2. SEC chromatograms of wild-type (WT) and mutants of fibulin 5. Chromatograms were base-line corrected and the differential refractive index (DRI, a measure of protein concentration) was normalized to 1.0 for each peak maximum. (**A–D**) Chromatograms for first applications to the SEC in the absence (**A**, buffer A) and presence (**B**, buffer B) of Ca^{2+}. (**A**) The peak maxima were aligned at 14 mL. The mean chromatogram (*line*) and confidence interval (*shaded area*) were calculated from chromatograms for three batches of WT. Duplicates are shown for G202R, C217R, and G412E. (**B**) The column void peak maxima were aligned at 8.25 mL. The mean chromatogram (*line*) was calculated from chromatograms for five batches of WT. The error bar shows the confidence interval for the position of the WT peak maximum. (**C**, **D**) Chromatograms for the reapplication of fractions from (**B**) (WT 13–13.5 mL, S227P 12–12.5 mL) to the SEC in the presence of Ca^{2+} so that molar masses (**C**) and R_H (**D**) could be determined without interference from light scattering at the column void.

fuge (Beckman Coulter, Hialeah, FL) equipped with an absorbance optical system. Sample and buffer were centrifuged in a two-sector centerpiece in an An-60 Ti 4-hole rotor at 45-krpm at 20°C. The sedimentation was monitored at 230 nm by 150 scans across a 1.4-cm radius with a step-size of 0.003 cm. Sedfit[25] performed Lamm equation boundary modeling to calculate size ($c(s)$) distributions, by using floated frictional ratios (f/f_0), and menisci positions, values for buffer densities and viscosities calculated with Sednterp,[26] and the estimate 0.7052 mL/g for the partial specific volume of the glycosylated recombinant fibulin 5 polypeptide.[16] Sednterp[26] then used sedimentation coefficients for $c(s)$ maxima to calculate f/f_0s, standard sedimentation coefficients ($S_{20,w}$), and hydrodynamic radii (R_H).

Circular Dichroism

CD is the differential absorption of left- and right-handed circularly polarized ultraviolet light. Spectra were measured between 190 and 260 nm by a J-810 spectropolarimeter (Jasco, Easton, MD) with a 0.05-cm path length, and an average of 10 scans; spectra were then baseline and buffer corrected. Different types of protein secondary structure (helix, strand, turn, and unordered) have signature spectra. Hence, the spectra were deconvoluted by the Dichroweb[27] server running the open-source CDSSTR software[28] with reference set 7 to provide estimates of the percentage of each secondary structure type.

RESULTS

Dimerization, Higher-Order Self-Association, and Mobility

Figure 2A shows the mean SEC chromatogram calculated for three batches of WT fibulin 5 and chromatograms for the mutants obtained in the absence of Ca^{2+}. The main peak maxima were aligned at 14 mL to compare peak shape. Lower molecular weight proteins elute later from the SEC at higher volumes. Between 10 and 12 mL, chromatograms for the mutants P87S, V126M, I169T, G202R, C217R, S227P, R351W, A363T, and G412E lay above the confidence interval (shaded gray) for WT, indicating increased self-association for these mutants ($P < 0.05$). At 10 mL both chromatograms for G412E showed the most deviation, indicating greatly increased self-association ($P < 0.001$). Both chromatograms for C217R formed a distinct second peak at 12.7 mL ($P < 0.005$) that mass-analysis showed was due to a dimer. The chromatograms for five other mutants (P87S, V126M, I169T, S227P, and R351W) gave points of inflection between 12 and 13 mL, probably because of small amounts of dimers. In addition, chromatograms for P87S, I169T, G202R, A363T, and G412E gave points of inflection at volumes <12 mL. Chromatograms (all shown in yellow in Fig. 2A and subsequent figures) for the mutants R54A, V60L, R71Q, Q124P, and G267S lay within the confidence interval for WT, suggesting that these mutations did not significantly affect the self-association of fibulin 5 in the absence of Ca^{2+}.

Figure 2B shows the mean SEC chromatogram calculated for five batches of WT fibulin 5 and chromatograms for the mutants obtained in the presence of Ca^{2+}. The column-void peaks (not shown) were aligned so that main peak positions could be compared. Ca^{2+} causes the main peaks to shift to the left, indicating more dimers and fewer monomers, and causes increased chromatogram height at lower volumes due to increased higher-order oligomerization.[16] The position of the peak maximum for S227P is outside the confidence interval (shown as the single black error bar, $P < 0.05$) for WT, suggesting increased self-association for S227P.

The chromatograms in Figures 2C and 2D illustrate the reapplication of SEC elution fractions (WT 13–13.5 mL, S227P 12–12.5 mL, shown in Fig. 2B) with the highest protein concentrations in the SEC in the presence of Ca^{2+} so that molar masses (Fig. 2C) and (Fig. 2D) could be determined easily. For WT, a dimeric molar mass (103 kDa) was approached only at the extreme left of the peak (Fig. 2C). For S227P, dimeric molar masses were measured across the whole peak (Fig. 2C), enabling us to obtain the estimate of 4.70 ± 0.04 nm for the radius for dimeric S227P (Fig. 2D).

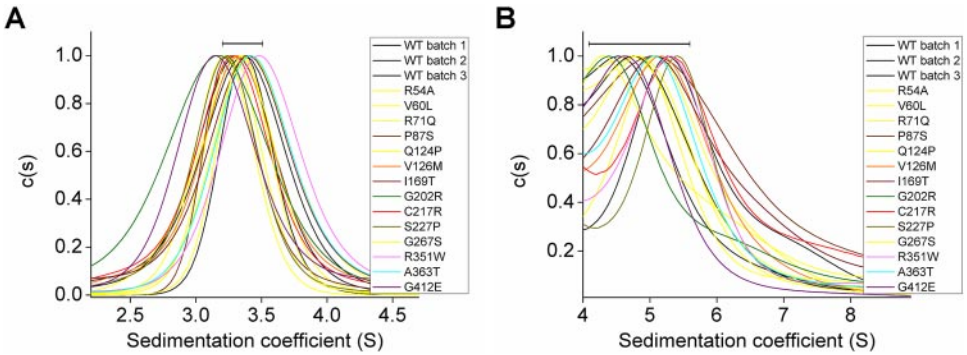

FIGURE 3. Velocity sedimentation of wild-type (WT) and mutants of fibulin 5 purified by SEC in the absence (**A**, buffer A) and presence (**B**, buffer B) of Ca $^{2+}$. Sedfit[25] provided the *c*(*s*) distributions. The horizontal error bars show the sedimentation coefficients within ±4.47 (**A**) and ±2 (**B**) SD of the three WT peak maxima.

The first chromatogram for G412E had the highest aggregation (measured by chromatogram height at ~10 mL) of 20 chromatograms measured when Ca^{2+} was absent (Fig. 2A). Also, the second chromatogram for G412E showed the highest aggregation of the other 19 chromatograms measured when Ca^{2+} was absent (Fig. 2A). Further, G412E gave the highest aggregation of 19 chromatograms measured in the presence of Ca^{2+} (Fig. 2B). We suggest that these results are dependent (i.e., not a coincidence) because the following calculation gave a low probability of their being independent (i.e., occurring by chance). Given that G412E had the highest aggregation in the absence of Ca^{2+}, the probability that independently G412E also has the second highest aggregation in the absence of Ca^{2+} and the highest aggregation in the presence of Ca^{2+} is (1/19) × (1/19) = 0.003. Further, G412E did not migrate as far toward the anode as R351W (which has a comparable electronegative substitution) during native (nondenaturing, nonreducing, pH 7.4, absence of Ca^{2+}) PAGE (Supplementary Fig. S2A).

Hydrodynamic Parameters

The monomeric and dimeric forms of the fibulin 5 mutants in the absence and presence of Ca^{2+} respectively underwent velocity sedimentation, and *c*(*s*) distributions for monomers (Fig. 3A) and dimers (Fig. 3B) were calculated by the program Sedfit.[25] Figure 3 shows confidence intervals (black error bars) calculated for the positions of the peak maxima for WT. The peak maxima for monomeric G202R and G412E lay outside the confidence interval for WT ($P < 0.05$, Fig. 3A). None of the peak maxima for the dimeric mutants were located outside the wide confidence interval calculated for WT in the presence of Ca^{2+} (Fig. 3B).

Table 1 shows f/f_0, $S_{20,w}$, and R_H calculated from the sedimentation velocity data (Fig. 3) for both monomeric and dimeric forms of the fibulin 5 mutants in the absence and presence of Ca^{2+}, respectively. The f/f_0 is a comparison of the shape of a protein to a sphere: The f/f_0 of a sphere is unity, whereas that of a linear protein is >1. The $S_{20,w}$ provides information about both the shape and the mass of the protein and has units of Svedbergs (S) where $1S = 10^{-13}$ seconds. Table 1 also shows the means (μ), standard errors (SE), and confidence intervals for the aforementioned parameters calculated from measurements for three batches of WT protein. Values for the hydrodynamic parameters for the mutants (G202R and G412E) that lie outside the confidence interval for WT ($P < 0.05$) are in italic (smaller values) or bold (larger values).

Analysis of Secondary Structure Content

CD is used to examine protein folding. Molar CD is expressed in units of delta epsilons. CD spectra (Fig. 4) were measured

TABLE 1. Hydrodynamic Parameters (Fig. 3) for Fibulin 5 Mutants Were Determined by Analysis of the Sedimentation Velocity Data

	Monomer*			Dimer†		
	f/f_0‡	$S^0_{20,w}$‡ $\times 10^{-13}$ s	R_H‡ nm	f/f_0‡	$S^0_{20,w}$‡$\times 10^{-13}$ s	R_H‡ nm
WT§						
Mean (μ)	1.48	3.73	3.61	1.64	5.35	5.04
± SE	± 0.01	± 0.02	± 0.02	± 0.07	± 0.25	± 0.23
± 4.47 SD	± 0.07	± 0.17	± 0.17	± 0.57	± 1.90	± 1.74
R54A	1.54	3.59	3.74	1.55	5.66	4.75
V60L	1.49	3.70	3.64	1.65	5.31	5.06
R71Q	1.51	3.64	3.69	1.69	5.18	5.19
P87S	1.53	3.60	3.73	1.57	5.57	4.82
Q124P	1.46	3.78	3.55	1.85	4.74	5.67
V126M	1.50	3.68	3.65	1.53	5.71	4.71
I169T	1.46	3.79	3.55	1.57	5.57	4.82
G202R	**1.56**	*3.53*	**3.81**	1.81	4.85	5.54
C217R	1.51	3.65	3.68	1.50	5.85	4.59
S227P	1.54	3.59	3.74	1.46	5.98	4.49
G267S	1.48	3.73	3.60	1.65	5.30	5.07
R351W	1.43	3.86	3.48	1.50	5.85	4.59
A363T	1.45	3.80	3.53	1.57	5.57	4.82
G412E	**1.58**	*3.50*	**3.84**	1.72	5.09	5.28

* Data for monomeric proteins were obtained in the absence of calcium (buffer A).

† Data for dimeric proteins were obtained in the presence of calcium (buffer B).

‡ Sednterp[26] used the MALLS-derived masses and the *S* values for *c*(*s*) maxima (Fig. 3) to calculate f/f_0, $S_{20,w}$, and R_H.

§ The mean (μ), SE, and 4.47 SD were calculated from results for three batches of WT protein. For the mutants, values $< \mu - 4.47$ SD (italic) and $> \mu + 4.47$ SD (bold) are indicated.

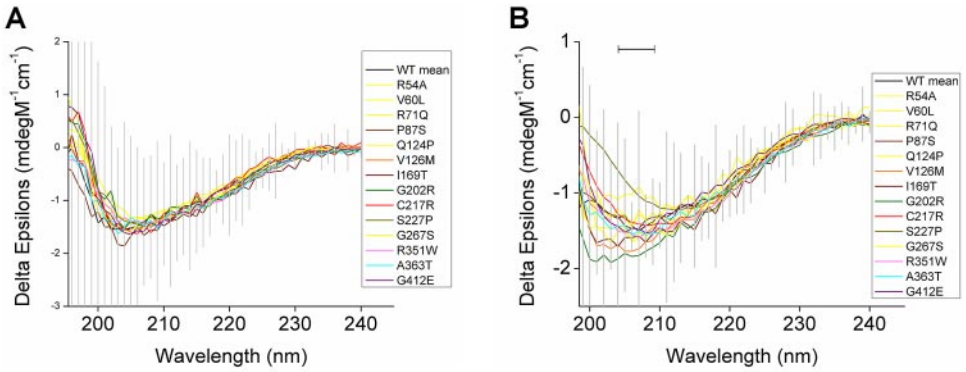

Figure 4. CD spectra of wild-type (WT) and mutants of fibulin 5 purified by SEC in the absence (**A**, buffer A) and presence (**B**, buffer B) of Ca^{2+}. The mean (*line*) and confidence interval (*hatched area*) for delta epsilons were calculated from spectra for three batches of WT. (**B**) The error bar shows the confidence interval for the wavelength of the WT delta epsilon minimum.

for the monomeric and dimeric forms of the fibulin 5 mutants in the absence and presence of Ca^{2+}, respectively. Figure 4 shows the mean spectrum (black line) and confidence interval (hatched area) calculated from CD spectra for three batches of WT in the absence and presence of Ca^{2+}. At lower wavelengths, the differences between the spectra measured in the absence of Ca^{2+} (Fig. 4A) were less than those measured in the presence of Ca^{2+} (Fig. 4B), indicating that Ca^{2+} interferes with measurements. The minimum in the spectrum measured for S227P in the presence of Ca^{2+} was shifted right to 212 nm, and lay outside the confidence interval (horizontal bar in Fig. 4B) for the WT minimum ($P < 0.05$). Deconvolution of the spectra provided estimates of secondary structure content (Table 2) for the monomeric and dimeric forms of the fibulin 5 mutants.

Homology Modeling

There are no high-resolution solved structures for any of fibulin 5's domains. However Figure 5A shows a putative arrangement of a fibulin 5 cbEGF based on the UniProt sequence for fibulin 5[15] and the consensus sequence for class I cbEGFs.[29] This arrangement could represent each of fibulin 5 cbEGF-2 to -6 but not the unusual cbEGF-1. In Figure 5A, the positions of mutations associated with cutis laxa and AMD that lie within fibulin 5 cbEGF-2 to -6 are shown on this representation of a single cbEGF.

The protein fold recognition program Threader 3.51[30] assessed whether the primary sequence for fibulin 5 WT cbEGF 4 (residues 206-246) could fold like the NMR structure (1EMN) for the fibrillin 1 cbEGF 33 domain.[29] The latter comprises the domain most homologous to fibulin 5 cbEGFs for which a high-resolution structure exists. Threading produced 98% alignment and 39% identity between the two sequences; all six cysteines in fibulin 5 cbEGF 4 were aligned with counterpart cysteines in fibrillin 1 cbEGF-33 (Supplementary Fig. S3). Swiss-Model[31] used this alignment to generate a (good) alignment of peptide backbones (Fig. 5B) and hence a putative homology model for fibulin 5 WT cbEGF 4 (Fig. 5C). Figure 5C shows the sites of the residues C217 (yellow) and S227 (blue) that are mutated in cutis laxa. No effect on the alignments or backbone structures was predicted by Swiss-Model[31] for the cutis laxa mutants C217R and S227P.

Discussion

Fibulin 5 is a calcium-binding protein of critical importance in the assembly of elastic fibers. Mutations in fibulin 5 have been shown to cause cutis laxa[11–13,32] and have been associated with AMD.[9,10] We used a combination of biophysical techniques to detect structural changes in these variants to help to determine the pathogenicity of the AMD-associated variants.

Table 2. Estimates from CD Spectra (Fig. 4) of the Secondary Structure Content of the Fibulin 5 Mutants

	Monomer*					Dimer†				
	NRMSD‡	Helix (%)	Strand (%)	Turn (%)	Unordered (%)	NRMSD‡	Helix (%)	Strand (%)	Turn (%)	Unordered (%)
WT§ mean (μ)	0.074	3.7	33.3	18.0	44.3	0.090	4.0	33.7	18.3	43.3
R54A	0.031	4	38	18	39	0.126	2	36	20	39
V60L	0.035	4	36	18	40	0.076	3	36	18	41
R71Q	0.034	6	34	19	40	0.065	4	37	18	40
P87S	0.066	4	34	18	43	0.047	4	35	18	43
Q124P	0.043	4	39	20	37	0.046	4	40	19	36
V126M	0.056	4	37	17	41	0.043	5	34	18	42
I169T	0.071	4	33	17	44	0.083	4	31	20	45
G202R	0.065	4	38	18	39	0.056	4	30	18	47
C217R	0.051	5	40	18	37	0.032	4	37	18	40
S227P	0.062	4	38	17	40	0.050	4	37	19	38
G267S	0.043	5	34	20	39	0.078	4	35	18	42
R351W	0.050	4	35	16	43	0.049	4	34	18	42
A363T	0.061	4	35	17	43	0.100	4	34	18	43
G412E	0.042	5	37	18	39	0.047	4	37	18	40

* Data for monomeric proteins were obtained in the absence of calcium (buffer A).
† Data for dimeric proteins were obtained in the presence of calcium (buffer B).
‡ The normalized root mean square deviation (NRMSD) is a measure of the fit of the data by the CDSSTR software[28] using reference set 7.
§ For comparison, the means (μ) were calculated from results for three batches of WT protein.

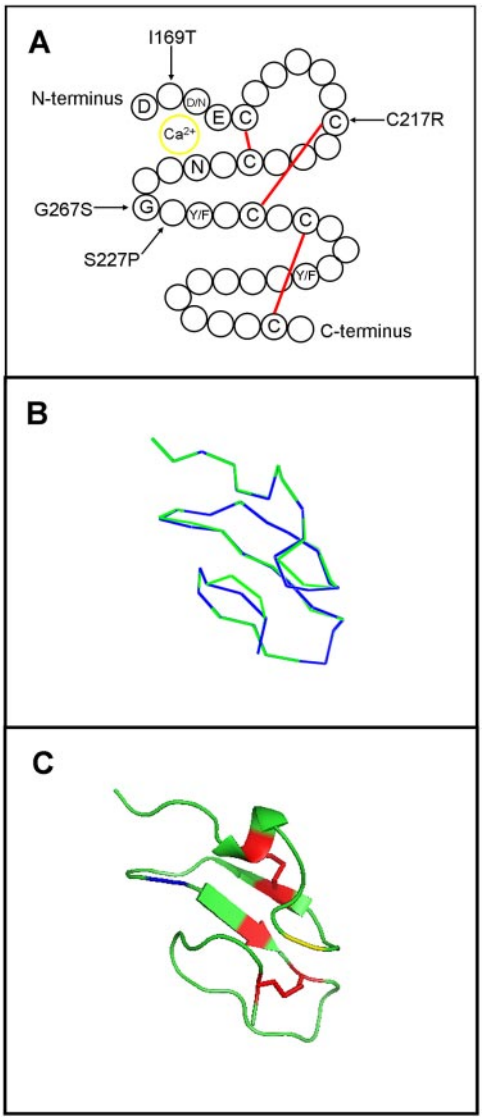

FIGURE 5. (**A**) Schematic putative arrangement of a normal fibulin 5 cbEGF that is based on the UniProt sequence for fibulin 5[15] and the consensus sequence for class I cbEGFs,[29] and that could represent each of fibulin 5 cbEGF-2 to -6, but not the abnormal cbEGF 1. Disulfide bonds are shown in red. Conserved residues are labeled using one-letter abbreviations. The positions of mutations associated with cutis laxa and AMD that lay within fibulin 5 cbEGFs 2 to 6 are shown on this representation of a single cbEGF. (**B**, **C**) Swiss-Model[31] used the alignments produced by threading (Supplementary Fig. S3) to generate (**B**) an alignment of peptide backbones for fibulin 5 cbEGF-4 (*green*) and fibrillin 1 cbEGF 33 (*blue*) and therefore (**C**) a putative homology model for fibulin 5 WT cbEGF 4. Cysteines and disulfide bonds are shown in *red* with the exceptions of residue C217 (*yellow*) and the disulfide bond (not shown) that is broken with the C217R mutation. *Blue*: the position of S227.

Results indicate that the two cutis laxa mutants (C217R and S227P) introduce differences in protein dimerization. C217R dimerizes more than the other mutants in the nonphysiological absence of Ca^{2+} (Fig. 2A). C217R removes a disulfide bond within cbEGF 4 (Fig. 5C), introduces a bulky charged arginine group, and is likely to reduce protein stability. S227P overdimerized in a Ca^{2+}-mediated reaction (Figs. 2B–D), and may perturb cbEGF 4's consensus calcium-binding sequence (Fig. 5A). This may result in S227P's reduced affinity for tropoelastin and fibrillin microfibrils.[33,34] Nonreduced SDS-PAGE showed that the dimerization of all mutants was not mediated by intermolecular disulfide bonds (Supplementary Fig. S2B). The AMD-associated mutant G412E gave the largest monomeric hydrodynamic radius, lower-than-expected mobility during native-PAGE, and greatly increased levels of higher-order self-association in SEC-MALLS experiments in both the presence and absence of Ca^{2+}. Together, these results suggest that G412E aggregates more than the other mutants. The increased dimerization of C217R and S227P and aggregation of G412E may explain their reduced secretion by COS7 cells.[9] It has been postulated that poor secretion leads to susceptibility to AMD.[9]

The three fibulin 5 mutations (R54A, V60L, and R71Q) closest to the integrin binding motif, Q124P and G267S had insignificant effects on the dimerization or aggregation of fibulin 5 in either the presence or absence of Ca^{2+}. With the exceptions of these and G412E, the mutations appear to slightly increase self-association of fibulin 5 in the absence of Ca^{2+}. However, that this property was exhibited by the G202R polymorphism suggests that a slight increase in self-association is not of strong predictive value when determining whether mutations cause disease. However, the G202R polymorphism is functionally different from WT because it increases binding to tropoelastin.[34,35]

We have presented and discussed CD spectra and estimates of secondary structure contents for WT fibulin 5 in both the absence and presence of Ca^{2+} previously.[16] CD spectra for the mutants (Fig. 4) resemble the mean spectra for three batches of WT acquired in each buffer, providing evidence that the mutants are folded into similar conformations. The spectrum measured for the cutis laxa mutation S227P in the presence of Ca^{2+} (Fig. 4B) appears to be different, with a minimum that is right-shifted to 212 nm. Although this difference is not supported by calculations of secondary structure content (Table 2), more weight should be placed on the actual data (Fig 4) and less on derived quantities.

Better solvation could explain why the chemically similar fibulin 5 substitutions V126M and G267S migrated farther toward the anode than did the WT during native PAGE (Supplementary Fig. S2A). Methionine and serine are more hydrophilic than the aliphatic residues that they replaced.[36] Threading predicted that the mutant G267S probably increases the solvation energy magnitude of fibulin 5.[9]

If we had performed these studies without the results of previous genetic studies, then we would have concluded that the two cutis laxa mutations and G412E are likely to be pathogenic. Although it remains uncertain as to whether G412E causes AMD, it is clear that our strategy detected differences for the two disease-causing cutis laxa mutations and was therefore of positive predictive value. Although the other AMD-associated mutants show no gross structural differences, the pathogenic mechanism of AMD may originate from the effects of subtle differences over a lifetime. Further, we cannot exclude the possibility that the AMD-associated mutants are pathogenic via differences outside the scope of this study—for example, intracellular effects or the disruption of intermolecular interactions.

Acknowledgments

The authors thank Adam Huffman (Department of Bioinformatics), Paul Fullwood (DNA Sequencing), Jemima Whyte and Stuart Cain (Faculty of Life Sciences), and Stephen Roberts (Faculty of Medical and Human Sciences), University of Manchester; Michael Harrison, University of Leeds, Julian Hanak (Renovo, Manchester, UK); Clive Kay (Vutrix, Weston Super Mare, UK); and Richard K. Jones.

References

1. Christen WG, Glynn RJ, Manson JE, Ajani UA, Buring JE. A prospective study of cigarette smoking and risk of age-related macular degeneration in men. *JAMA.* 1996;276:1147–1151.
2. Seddon JM, Willett WC, Speizer FE, Hankinson SE. A prospective study of cigarette smoking and age-related macular degeneration in women. *JAMA.* 1996;276:1141–1146.
3. Gold B, Merriam JE, Zernant J, et al. Variation in factor B (BF) and complement component 2 (C2) genes is associated with age-related macular degeneration. *Nat Genet.* 2006;38:458–462.
4. Edwards AO, Ritter R, Abel KJ, Manning A, Panhuysen C, Farrer LA. Complement factor H polymorphism and age-related macular degeneration. *Science.* 2005;308:421–424.
5. Hageman GS, Anderson DH, Johnson LV, et al. A common haplotype in the complement regulatory gene factor H (HF1/CFH) predisposes individuals to age-related macular degeneration. *Proc Natl Acad Sci U S A.* 2005;102:7227–7232.
6. Haines JL, Hauser MA, Schmidt S, et al. Complement factor H variant increases the risk of age-related macular degeneration. *Science.* 2005;308:419–421.
7. Klein RJ, Zeiss C, Chew EY, et al. Complement factor H polymorphism in age-related macular degeneration. *Science.* 2005;308:385–389.
8. Rivera A, Fisher SA, Fritsche LG, et al. Hypothetical LOC387715 is a second major susceptibility gene for age-related macular degeneration, contributing independently of complement factor H to disease risk. *Hum Mol Genet.* 2005;14:3227–3236.
9. Lotery AJ, Baas D, Ridley C, et al. Reduced secretion of fibulin 5 in age-related macular degeneration and cutis laxa. *Hum Mutat.* 2006;27:568–574.
10. Stone EM, Braun TA, Russell SR, et al. Missense variations in the fibulin 5 gene and age-related macular degeneration. *N Engl J Med.* 2004;351:346–353.
11. Elahi E, Kalhor R, Banihosseini SS, et al. Homozygous missense mutation in fibulin-5 in an Iranian autosomal recessive cutis laxa pedigree and associated haplotype. *J Investig Dermatol.* 2006;126:1506–1509.
12. Fischer J, Jobard F, Oudot T, et al. Identification of novel mutations in elastin and fibulin 5 in three patients affected with cutis laxa. Presented at the Third European Symposium on Elastin. Manchester, UK, June 30–July 3, 2004.
13. Loeys B, Van Maldergem L, Mortier G, et al. Homozygosity for a missense mutation in fibulin-5 (FBLN5) results in a severe form of cutis laxa. *Hum Mol Genet.* 2002;11:2113–2118.
14. Timpl R, Sasaki T, Kostka G, Chu ML. Fibulins: a versatile family of extracellular matrix proteins. *Nat Rev Mol Cell Biol.* 2003;4:479–489.
15. Reviewed US-P. Q9UBX5 (FBLN5_HUMAN). http://wwwuniprotorg/uniprot/Q9UBX5 2009.
16. Jones RPO, Wang MC, Jowitt TA, et al. Fibulin 5 forms a compact dimer in physiological solutions. *J Biol Chem.* 2009; 284(38): 25938–25943.
17. de Vega S, Iwamoto T, Yamada Y. Fibulins: Multiple roles in matrix structures and tissue functions. *Cell Mol Life Sci.* 2009;66(11–12): 1890–1902.
18. Kowal RC, Richardson JA, Miano JM, Olson EN. EVEC, a novel epidermal growth factor-like repeat-containing protein upregulated in embryonic and diseased adult vasculature. *Circ Res.* 1999; 84:1166–1176.
19. Nakamura T, Ruiz-Lozano P, Lindner V, et al. DANCE, a novel secreted RGD protein expressed in developing, atherosclerotic, and balloon-injured arteries. *J Biol Chem.* 1999;274:22476–22483.
20. Nakamura T, Lozano PR, Ikeda Y, et al. Fibulin-5/DANCE is essential for elastogenesis in vivo. *Nature.* 2002;415:171–175.
21. Yanagisawa H, Davis EC, Starcher BC, et al. Fibulin-5 is an elastin-binding protein essential for elastic fibre development in vivo. *Nature.* 2002;415:168–171.
22. Freeman LJ, Lomas A, Hodson N, et al. Fibulin-5 interacts with fibrillin-1 molecules and microfibrils. *Biochem J.* 2005;388:1–5.
23. Lomas AC, Mellody KT, Freeman LJ, Bax DV, Shuttleworth CA, Kielty CM. Fibulin-5 binds human smooth-muscle cells through alpha5beta1 and alpha4beta1 integrins, but does not support receptor activation. *Biochem J.* 2007;405:417–428.
24. Dixon WJ, Massey FJ. *Introduction to Statistical Analysis*. New York: McGraw Hill; 1983;:44–152, 400–401, 534.
25. Schuck P. Size-distribution analysis of macromolecules by sedimentation velocity ultracentrifugation and Lamm equation modeling. *Biophys J.* 2000;78:1606–1619.
26. Hayes D, Laue T, Philo J. Program Sednterp: sedimentation interpretation program. Durham, NH: University of New Hampshire; 1995.
27. Whitmore L, Wallace BA. DICHROWEB, an online server for protein secondary structure analyses from circular dichroism spectroscopic data. *Nucleic Acids Res.* 2004;32:W668–W673.
28. Compton LA, Johnson WC. Analysis of protein circular-dichroism spectra for secondary structure using a simple matrix multiplication. *Anal Biochem.* 1986;155:155–167.
29. Downing AK, Knott V, Werner JM, Cardy CM, Campbell ID, Handford PA. Solution structure of a pair of calcium-binding epidermal growth factor-like domains: implications for the Marfan syndrome and other genetic disorders. *Cell.* 1996;85:597–605.
30. Jones DT, Tress M, Bryson K, Hadley C. Successful recognition of protein folds using threading methods biased by sequence similarity and predicted secondary structure. *Proteins Struct Funct Genet.* 1999(suppl 3);104–111.
31. Arnold K, Bordoli L, Kopp J, Schwede T. The Swiss-Model workspace: a web-based environment for protein structure homology modelling. *Bioinformatics.* 2006;22:195–201.
32. Markova D, Zou Y, Ringpfeil F, et al. Genetic heterogeneity of cutis laxa: a heterozygous tandem duplication within the fibulin-5 (FBLN5) gene. *Am J Hum Genet.* 2003;72:998–1004.
33. Hu Q, Loeys BL, Coucke PJ, et al. Fibulin-5 mutations: mechanisms of impaired elastic fiber formation in recessive cutis laxa. *Hum Mol Genet.* 2006;15:3379–3386.
34. Choudhury R, McGovern A, Ridley C, et al. Differential regulation of elastic fiber formation by fibulins-4 and -5. *J Biol Chem.* 2009; 284(36):24553–24567.
35. Hu QR, Reymond JL, Pinel N, Zabot MT, Urban Z. Inflammatory destruction of elastic fibers in acquired cutis laxa is associated with missense alleles in the elastin and fibulin-5 genes. *J Investig Dermatol.* 2006;126:283–290.
36. Mathews CK, Van Holde KE. *Biochemistry*. Reading, MA: Benjamin/Cummings. 1990:xxix,1129.